



## Strathprints Institutional Repository

Halling, P.J. (2009) *Estimation of flattening coefficient for absorption and circular dichroism using simulation*. Analytical Biochemistry, 387 (1). pp. 76-81. ISSN 0003-2697

Strathprints is designed to allow users to access the research output of the University of Strathclyde. Copyright © and Moral Rights for the papers on this site are retained by the individual authors and/or other copyright owners. You may not engage in further distribution of the material for any profitmaking activities or any commercial gain. You may freely distribute both the url (<http://strathprints.strath.ac.uk/>) and the content of this paper for research or study, educational, or not-for-profit purposes without prior permission or charge.

Any correspondence concerning this service should be sent to Strathprints administrator: <mailto:strathprints@strath.ac.uk>

Halling, P.J. (2009) Estimation of flattening coefficient for absorption and circular dichroism using simulation. *Analytical Biochemistry*, 387 (1). pp. 76-81. ISSN 0003-2697

<http://strathprints.strath.ac.uk/19249/>

This is an author produced version of a paper published in *Analytical Biochemistry*, 387 (1). pp. 76-81. ISSN 0003-2697. This version has been peer-reviewed but does not include the final publisher proof corrections, published layout or pagination.

Strathprints is designed to allow users to access the research output of the University of Strathclyde. Copyright © and Moral Rights for the papers on this site are retained by the individual authors and/or other copyright owners. You may not engage in further distribution of the material for any profitmaking activities or any commercial gain. You may freely distribute both the url (<http://strathprints.strath.ac.uk>) and the content of this paper for research or study, educational, or not-for-profit purposes without prior permission or charge. You may freely distribute the url (<http://strathprints.strath.ac.uk>) of the Strathprints website.

Any correspondence concerning this service should be sent to The Strathprints Administrator: [eprints@cis.strath.ac.uk](mailto:eprints@cis.strath.ac.uk)

Preprint of article published in *Analytical Biochemistry* **387**: 76–81.

DOI: 10.1016/j.ab.2009.01.006

## **Estimation of flattening coefficient for absorption and circular dichroism using simulation**

Peter J Halling

WestCHEM, Dept Pure & Applied Chemistry, University of Strathclyde, Glasgow G1 1XL,  
UK

P.J.Halling@strath.ac.uk

Tel: +44 141 548 2683

Fax: +44 141 548 4822

Short title: Simulation of absorption and CD flattening

## **ABSTRACT.**

The absorbance and circular dichroism (CD) of suspensions is lower than if the same amount of chromophore were uniformly distributed throughout the medium. Several mathematical treatments of this absorption flattening phenomenon have been presented, using various assumptions and approximations. This paper demonstrates an alternative simulation approach, which allows relaxation of assumptions. On current desk-top computers the algorithm runs quickly with enough particles and light paths considered to get answers usually accurate to better than 3%. Results from the simulation agree with the most popular analytical model for 0.01 volume fraction of particles, showing that the extent of flattening depends mainly on the absorbance through a particle diameter. Unlike previous models, the simulation can show that flattening is significantly lower when volume fraction increases to 0.1, but higher if the particles have a size distribution. The simulation can predict the slope of the nearly linear relationship between flattening of CD and the absorbance of the suspension. This provides a method to correct experimental CD data, where volume fraction and particle size are known.

Keywords: protein particles, particle size, software

## **INTRODUCTION.**

Measurements of light absorption or circular dichroism on suspended particles may differ compared with the same amount of chromophore uniformly distributed in solution. A key contribution is the phenomenon of absorption flattening, which has in the past also been termed “shadowing”, “obscuring” and the “sieve effect” [1-14]. (The instrument signal may also be affected by light scattering, which will not be considered further in this paper.) There are several different pictures of the origin of the flattening effect, but all of them relate to the same fundamental cause. Perhaps the easiest is to imagine the appearance of a projection of the suspension in a plane perpendicular to the light path (i.e. as seen by the light entering the suspension). Now, if the particles are sufficiently dilute, there will be parts of this projection that contain no particles at all (i.e. light paths through the suspension that pass entirely through the transparent suspending medium). Fig. 1 below shows examples. Now it should be clear that the suspension will have a minimum transmittance, even if the particles completely

absorb light meeting them. Hence the suspension will have a maximum absorbance, however large the chromophore concentration within the particles or its absorbance coefficient. A slightly different picture considers that because of the random distribution of particles, different light paths through the suspension will pass through particles for different fractions of their length. The average of the absorbance over these various paths will equal that if the same amount of chromophore were uniformly distributed. But the spectrophotometer will average not absorbances but intensities (which are exponential functions of the former). The smaller absorbance (larger intensity) paths will make a disproportionately large contribution to this mean intensity. Hence the final absorbance calculated from the mean intensity will be smaller than the mean absorbance, unless the absorbances through each light path are exactly equal.

If all absorbances are relatively small, it is fairly easy to see that the absorbance reducing effects of the high transmittance light paths (meeting few or no particles) will be weaker. Hence the effect most strongly reduces measured absorbance in regions of the spectrum where the absorbance coefficient is high, flattening the tops of the peaks (the origin of the name).

The same phenomenon also affects circular dichroism (CD) spectra, because these show the difference in absorbance for right and left circularly polarised light. Indeed, there has been more interest recently in flattening effects in CD than for simple absorbance. In part this is because in CD light scattering from suspensions has a smaller impact - simple light scattering (of equal magnitude for both polarisations) does not affect the CD signal, provided sufficient light still reaches the detector for it to be measured. Measurements of circular dichroism on suspensions have been widely used in the study of membrane proteins. These must normally be kept in place in membrane fragments in order to retain their native structures. Flattening effects can be significant when measurements are made on the resulting suspensions [5,7,15]. CD measurements are also of interest on other types of small particles in suspension (e.g. [16,17]).

It has recently been shown possible to collect good circular dichroism data on suspensions of particles of hundreds of  $\mu\text{m}$  in size [11]. This opens the possibility of examining protein conformation in a wide variety of particulate preparations of practical interest, including immobilised enzymes [18], various dried storage forms [19], and the results of unwanted aggregation in solution [20].

The size of the flattening effect was first analysed in a classic paper by Duysens [1]. Since then there have been a series of approaches to modelling the effect [2-14], which are discussed in more detail in the Theory section. The literature approaches have used analytical treatments to derive equations that describe the effect, with the use of various simplifying or approximating assumptions. The final equations may be solved analytically or numerically, and their predictions are shown below for comparison. In this paper I will describe and present results from a simulation approach to describe the phenomenon. This would have been computationally extremely expensive or impossible at the time of most of the previous treatments. However, as will be shown, the speed of current computers makes it an attractive option. A simulation approach also makes it relatively easy to relax one or more of the approximations made in relation to the real system.

## THEORY

### Simulation approach

The basic idea is to simulate the passage of light along the full pathlength through a portion of the sample volume. The appropriate number of particles are placed randomly within the volume, and then an array of possible light paths are examined. For each light path, calculate the fraction of its length that passes through one or more particles, and hence determine the intensity of light that would emerge from that path. From the summed intensities the expected measured absorbance or CD signal of the suspension can be calculated. This may be compared with the values that would be found if the chromophores were distributed uniformly through the medium (or, equivalently, when every light path had an identical fraction of its length within the particles, equal to their volume fraction).

The appearance of the suspension in a projection perpendicular to the light path does not depend on the absolute pathlength, but rather on its ratio to the particle diameter (see examples in Fig. 1). Hence it is convenient to use a dimensionless parameter ( $L$ ), the pathlength divided by the particle diameter, to characterise the system. The volume fraction of the particles in the suspension ( $\phi$ ), also dimensionless, is another input to the simulation. The absorption within the particles will depend on the concentration of chromophore within them multiplied by its absorption coefficient. Again it is convenient, and parallels previous

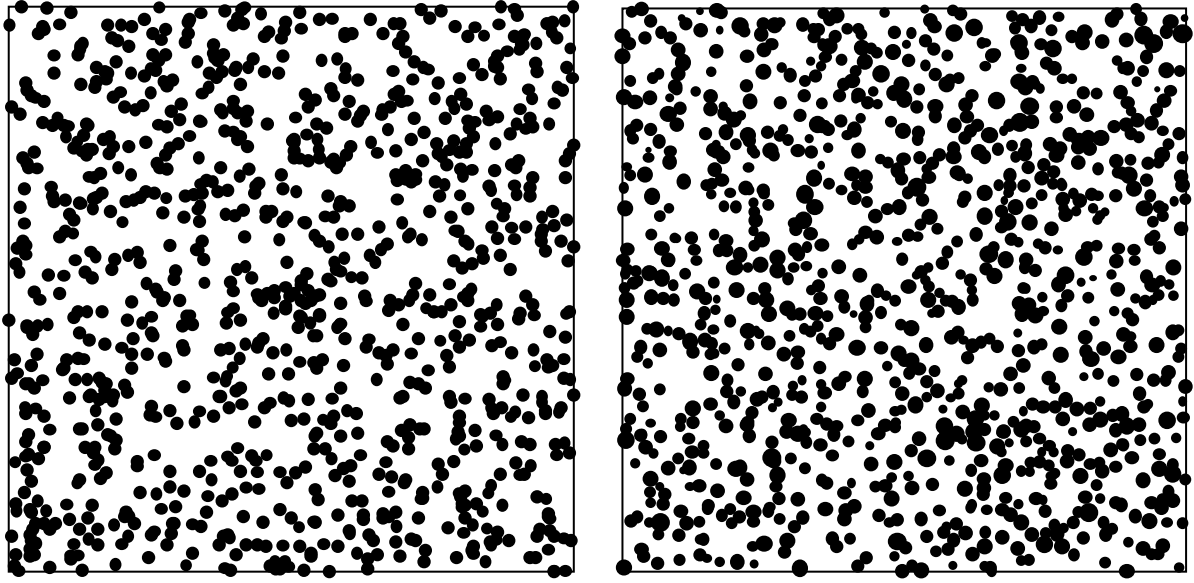


Fig. 1. Simulated appearance of suspension as viewed along light path. Left panel, for  $\phi = 0.01$  and  $L = 20$ ; right panel, for  $\phi = 0.1$  and  $L = 2$  with a 20% standard deviation in particle diameters. It is evident that many light rays will not meet any particle at all. The calculated maximum absorbances of the suspension are about 0.13 and 0.15, however large  $A_{\text{part}}$  becomes.

analytical treatments, to make this dimensionless by multiplying by the particle diameter. The result, which is equal to the absorbance measured through a diameter of the particle, is denoted by  $A_{\text{part}}$ . To simulate the effect on CD measurements, we use the corresponding CD signal for a light ray that passes through the diameter of one particle,  $CD_{\text{part}}$ . This is by definition equal to  $A_{\text{part,L}} - A_{\text{part,R}}$ , the difference in absorbances for left and right circularly polarised light. To find the individual terms, we make use of the fact that the average intensity transmitted by the particle (as appearing in the definition of  $A_{\text{part}}$ ) is equal to the mean of transmitted intensities of the two polarisations. This allows us to derive:

$$A_{\text{part,L}} = A_{\text{part}} + \log\left(\frac{1 + 10^{CD_{\text{part}}}}{2}\right) \quad A_{\text{part,R}} = A_{\text{part}} + \log\left(\frac{1 + 10^{-CD_{\text{part}}}}{2}\right)$$

Because all four inputs to the simulation are dimensionless, all lengths considered in the simulation will also be dimensionless multiples of the particle diameter.

The simulation then proceeds as follows:

1. Set up a simulated volume, with pathlength  $L$ , which will be taken as the  $z$ -axis direction. The total volume ( $V$ ) is chosen to contain the number of particles to be included in the simulation ( $N$ , e.g. 1000), by  $V = N \cdot \pi / (6 \cdot \phi)$ . Note that the value of  $N$  does not affect the nature of the system being simulated (which depends only on  $\phi$  and  $L$ ), but just the size of the portion that is included in the simulation.  $N$  must be large enough that this portion is representative of the system as a whole. Note also that  $V$  will also be dimensionless, based on division by the cube of the particle diameter. To achieve the required volume, equal widths of the simulation region are then set in the  $x$  and  $y$  directions ( $=\sqrt[3]{(V/L)}$ ).
2. Place the required number of spherical particle centres randomly throughout the simulated volume, not allowing a new particle to overlap a previous one, or to overlap the ends of the volume in the  $z$  direction (assumed to be sample container walls). Overlap of the simulation volume edges in the  $x$  and  $y$  directions are allowed, as these are merely arbitrarily chosen limits to the simulation volume.
3. Consider an array of light ray paths along the  $z$  direction, uniformly distributed in the  $x$ - $y$  plane (e.g. 32 X 32 raster, giving a total of 1024). For each light ray, calculate the total length of its path through particles. The algorithm does this by simply considering each simulated particle in turn, seeing if it intersects that ray. For a light ray that has coordinates  $x_r$  and  $y_r$  such that it passes through a particle of radius  $R$ , at a distance  $r$  from the particle centre ( $=\sqrt{[(x_r-x_p)^2+(y_r-y_p)^2]}$ ), the light path length through the particle is  $2\sqrt{(R^2-r^2)}$ . (This neglects refraction at the particle-medium surface.) All such contributions to the given light ray are summed. Light paths are placed at least one particle radius from the  $x$  and  $y$  edges, so they could not meet any particles centred outside the simulated volume.
4. For each light ray, and a list of possible values of  $A_{\text{part}}$ , calculate an absorbance as  $A_{\text{part}}$  times the total path length through particles (remembering that this path length is calculated as a multiple of particle diameter). Then calculate the transmitted fractions of light intensity for that light ray as 10 raised to the negative power of absorbance. The transmittance of right and left polarised light are calculated similarly using  $A_{\text{part,L}}$  and  $A_{\text{part,R}}$  (calculated from input values of  $A_{\text{part}}$  and  $CD_{\text{part}}$ ).



5. Calculate the average transmitted intensity from all these light paths, for each possible combination of  $A_{\text{part}}$  and  $CD_{\text{part}}$  values, and hence the (flattened) absorbances of the suspension ( $A_{\text{sus}}$ ). Calculate the CD signal of the suspension ( $CD_{\text{sus}}$ ) as the difference in  $A_{\text{sus}}$  values for left and right polarised light.
6. Calculate the reference absorbance ( $A_{\text{sol}}$ ) or CD signal ( $CD_{\text{sol}}$ ) if the absorbing material were uniformly distributed (no flattening). First calculate the average across all light paths of the path length through particles. This should be very close to the product  $\phi.L$ , and is found to be so, although the random element in the simulation means they differ slightly. Then multiply by the various possible  $A_{\text{part}}$  or  $CD_{\text{part}}$  values.
7. For the estimation of the flattening coefficient ( $Q_A$ ) as  $A_{\text{sus}}/A_{\text{sol}}$ , the  $A_{\text{sol}}$  values might be calculated as  $A_{\text{part}}$  multiplied either by  $\phi.L$ , or by the average path length through particles (as under step 6). The  $Q_A$  values from replicate simulations were found to be rather closer to each other using the latter approach. The same applied to  $Q_{CD}$  values, calculated as  $CD_{\text{sus}}/CD_{\text{sol}}$ . Hence the latter approach has been used to give the results shown here. The random element in the simulation results in a set of light ray paths that have a slightly larger or smaller average length in particles. Essentially this means they are characteristic of a slightly different value of  $\phi$ , compared with that input.

A number of assumptions and approximations are made in this treatment, but it should be possible to relax these, at the expense of a more complicated calculation.

- The current simulation treats light passage through the suspension in terms of classical geometric optics. As such it will not be valid in cases where the particles sizes are not significantly larger than the wavelengths of the light used [4, 8].
- Light paths are treated as straight lines all though the suspension, neglecting possible refraction at the particle surfaces.
- It is assumed the chromophore is equally distributed between the particles, and evenly distributed within each.

The algorithm would also need altering to handle particles of different shape (e.g. cylinders or hollow spheres), or to deal with a range of particle sizes. As an illustration of the possibilities,

the last of these is demonstrated below. Other extensions are under development. To get reliable results for the more complicated cases it may be necessary to include more particles and/or light paths in the simulation, with a corresponding increase in calculation time.

### **Re-arrangement and re-parameterisation of literature equations for comparison**

In order to compare the results of the simulation approach with those from literature equations, it is necessary to convert these to use the same dimensionless input variables (i.e.  $A_{\text{part}}$ ,  $\phi$  and  $L$ ). One useful relationship here is that  $A_{\text{sol}} = A_{\text{part}} \cdot \phi \cdot L$ , since other treatments show the relationship of  $A_{\text{sol}}$  to their input values.

A series of papers derive essentially the same equation by different routes and arguments [1-4, 10]. Using the symbols of Naqvi et al [10], the procedure is to calculate first the parameter  $\alpha$ , by

$$\alpha = \varepsilon \cdot n \cdot d \cdot \ln 10 \quad (1)$$

where  $\varepsilon$  is the extinction (absorbance) coefficient of the chromophore,  $n$  is its concentration within the particle and  $d$  is the particle diameter. It is clear that  $\alpha$  equals  $A_{\text{part}}$  as defined above multiplied by  $\ln 10$ . The factor of  $\ln 10$  appears because the treatment essentially specified absorbance as  $\ln(I_0/I)$ , which is indeed used as its definition in the earlier papers, rather than  $\log(I_0/I)$  as standard nowadays. From  $\alpha$ , calculate  $\beta$ , the ‘‘average transmission of a particle’’, as

$$\beta = \frac{2[1 - (1 + \alpha)e^{-\alpha}]}{\alpha^2} \quad (2)$$

Finally, calculate  $Q_A$  ( $A_D/A_C$  in their symbols) by

$$Q_A = \frac{A_D}{A_C} = \frac{3(1 - \beta)}{2\alpha} \quad (3)$$

Hence the model predicts that  $Q_A$  depends only on  $A_{\text{part}}$ , and is independent of  $\phi$  and  $L$ . Some of the derivations explicitly assume that  $\phi \ll 1$ .

Wittung et al [9] show a derivation with the final equation printed as:

$$A_{sus} = \frac{1}{\sigma\sqrt{2\pi}} \sum_{n=0}^{N_p} e^{-\frac{(n-\mu)^2}{2\sigma^2}} \cdot 10^{-n \cdot \frac{N_{ch}}{N_p} \varepsilon_p \cdot c_p \cdot l} \quad (4)$$

with  $\mu = \frac{N_p}{N_{ch}}$  and  $\sigma = \sqrt{\frac{N_p}{N_{ch} \left(1 - \frac{1}{N_{ch}}\right)}} \approx \sqrt{\frac{N_p}{N_{ch}}}$

However, examination of their derivation shows that the expression actually gives  $I_{sus}/I_o$ , so  $A_{sus}$  should be calculated as the negative log of this value. In this equation:

$N_p$  is the total number of particles in the sample cell

$N_{ch}$  is the number of light “channels” through the sample – these are to be chosen so they have “a cross-section corresponding to the size of the absorbing particles”.

$\varepsilon_p$  is the “molar absorptivity of the particles”

$c_p$  is the “molar concentration of the particles”

$l$  is the sample pathlength

One stated limit on validity is that  $N_p/N_{ch} > 2$ .

To relate this equation to the input values used in the simulation, we introduce (and later cancel) the area  $A$  of the suspension in the x-y plane, facing the light beam. Now we can interpret the rule stated above for choosing channel size as meaning  $N_{ch} = A/d^2$ , where  $d$  is the particle diameter. (An alternative interpretation would be  $N_{ch} = 4A/\pi d^2$ , giving slightly different relationships.) We can also write  $N_p = n_p \cdot A \cdot l$ , where  $n_p$  is the number of particles per unit volume in the suspension. But  $n_p$  can also be related to  $\phi$  by  $\phi = n_p \cdot \pi d^3/6$ . Hence we obtain  $N_p/N_{ch} = (6/\pi) \cdot \phi \cdot L$ . Wittung et al [9] also present the relationship  $A_{sol} = \varepsilon_p \cdot c_p \cdot l$ , so we can replace the entire group  $(N_{ch}/N_p) \cdot \varepsilon_p \cdot c_p \cdot l$  by  $\pi \cdot A_{part}/6$ . Hence we calculate  $Q_A$  by

$$Q_A = \frac{A_{sus}}{A_{sol}} = \frac{1}{A_{part} \cdot \phi \cdot L} \cdot -\log \left[ \frac{1}{\sigma\sqrt{2\pi}} \sum_{n=0}^{N_p} e^{-\frac{(n-\mu)^2}{2\sigma^2}} \cdot 10^{-\frac{n \cdot \pi \cdot A_{part}}{6}} \right] \quad (5)$$

$$\text{with } \mu = \frac{6 \cdot \phi \cdot L}{\pi} \quad \text{and} \quad \sigma = \sqrt{\frac{6 \cdot \phi \cdot L}{\pi \cdot \left(1 - \frac{1}{N_{ch}}\right)}} \approx \sqrt{\frac{6 \cdot \phi \cdot L}{\pi}} \quad \text{and} \quad N_p = \frac{6 \cdot \phi \cdot L \cdot N_{ch}}{\pi}$$

Thus  $Q_A$  is predicted to depend on  $A_{\text{part}}$ ,  $\phi \cdot L$ , and  $N_{\text{ch}}$ . The stated limit on validity becomes  $\phi \cdot L > 1$ . For the  $A_{\text{part}}$  and  $\phi \cdot L$  ranges studied, the influence of  $N_{\text{ch}}$  was found to be small when it is greater than 20.

Bustamante and Maestre [8] derive the following equations (their 12, and the following expression for  $q$ , using their 11 to expand  $V_f$ ):

$$Q_A = \frac{A_{\text{sus}}}{A_{\text{sol}}} = 1 - \left[ \frac{2.303 \cdot a(1-q)}{2 \cdot k \cdot \lambda^2} \right], \quad \text{with} \quad q = \frac{W \cdot N_a \cdot k \cdot \lambda^2 \cdot l}{M_w \cdot V_T} \quad (6)$$

where

$a$  is the absorption cross section of the chromophore, with dimensions of length squared

$q$  is “the probability of finding a particle in the volume defined by a light pencil”

$k$  is a “proportionality constant whose exact value is of no consequence”, which they take as 1

$\lambda$  is the wavelength of the light used

$W$  is the total weight of the absorbing material in the solution

$N_a$  is Avogadro’s number

$l$  is the pathlength

$M_w$  is the molecular weight of the absorbing particles

$V_T$  is the total volume of the solution

The identification of  $q$  as a probability implies a maximum value of 1, and hence a limit on the validity of the expression that gives it. We can also simplify this expression by replacing  $W \cdot N_a / (M_w \cdot V_T)$  with  $c$ , the number of particles per unit volume (as used earlier in their derivation). We also have  $A_{\text{sol}} = a \cdot c \cdot l$  (as used in their derivation), but also  $A_{\text{sol}} = A_{\text{part}} \cdot \phi \cdot L$ , from above. Hence we obtain

$$Q_A = 1 - \left( \frac{2.303 \cdot A_{part} \cdot L \cdot \phi}{2} \right) \left( \frac{1}{k \cdot \lambda^2 \cdot l \cdot c} - 1 \right) \quad (7)$$

Thus  $Q_A$  is predicted to depend on the two dimensionless groups  $A_{part} \cdot \phi \cdot L$  and  $k \cdot \lambda^2 \cdot l \cdot c$ , where one limit to validity is that the latter must be less than 1.

There are fewer equations in the literature for flattening of CD spectra of spherical particles. Gordon & Holzwarth [2] present

$$Q_{CD} = Q_B = \frac{2 \cdot q \cdot m}{A_{sol}} \left[ T_p - \exp\left(-\frac{3 \cdot A_{sol}}{2 \cdot q \cdot m}\right) \right] \quad (8)$$

where  $q$  is the volume fraction of particles (i.e.  $\phi$ ),  $m = (3 \times \text{pathlength}) / (4 \times \text{particle radius})$  (i.e.  $3L/2$ ), and  $T_p$  is an alternative symbol for  $\beta$  calculated as in equation 2 above.

Substitution leads to

$$Q_{CD} = \frac{3}{\alpha} [\beta - \exp(-\alpha)] \quad (9)$$

Urry [3] presents an algorithm for the calculation of  $Q_{CD}$ , by successive use of equations 44 and 45, 46, 47 and 42 (as numbered in that paper). For comparison with the present treatment, the scattering terms in equation 42 are set to zero. The input values to the algorithm are  $A_{part}$ ,  $CD_{sol}$  and  $A_{sol}$  (using my symbols). However, a test using a range of realistic values indicates that the latter two have almost no effect on the calculated  $Q_{CD}$ . Furthermore, the  $Q_{CD}$  values obtained are found to agree within 0.1% with those calculated using equation 9 above. Hence they are not treated separately below.

Bustamante and Maestre [8] derive the relationship:

$$Q_{CD} = 2(Q_A - 0.5) \quad (10)$$

where  $Q_A$  is obtained from their equation 6 (or 7) as given above.

## RESULTS AND DISCUSSION

The simulation has been implemented as a Visual Basic macro attached to an Excel spreadsheet. The latest version of this will be supplied without restriction on request to the author. Running a simulation with 1000 particles and 1024 light paths takes about 3 s on a standard PC. Replicate simulations with these values usually agree with standard deviations in  $Q_A$  and  $Q_{CD}$  values of <3%, often much smaller. Larger deviations are observed in some cases, especially where the values of  $A_{sus}$  are very large, or  $Q_{CD}$  is very small. Standard deviations are shown as error bars on the graphs presented (often smaller than the points). Increasing the number of particles to 5000 seemed to have little effect on the standard deviations obtained, whereas an increase to 4098 (64 X 64) light paths typically reduced the standard deviation to about half.

Simulations have been run for input values in the following ranges:  $A_{part}$  0.001 to 5;  $\phi$  0.01 to 0.1;  $L$  2 to 2000;  $CD_{part}$  0.00001 to 0.1 (and no more than 10% of  $A_{part}$ ). The effects of  $\phi$ ;  $L$  and  $CD_{part}$  on  $Q_A$  and  $Q_{CD}$  are found to be relatively small, with  $A_{part}$  having the major influence. Fig. 2 shows the dependency of  $Q_A$ , with simulation results indicated by points. For comparison, lines show the predictions of the 3 literature models above. As can be seen, the simulation points for  $\phi = 0.01$  agree well with equation 3, as might be expected in the low  $\phi$  limit. For  $\phi = 0.1$  the values of  $Q_A$  obtained by simulation are slightly but significantly larger (i.e. less flattening). One contributing effect here is the greater restriction on particle locations by others present in the suspension (i.e. an excluded volume effect). This makes the distribution of particles across light paths rather more uniform as  $\phi$  increases. It may be helpful to think of behaviour at very high  $\phi$ , approaching the close packed limit, when the particle centres must be arranged ever closer to a regular lattice.

The model of equations 4 and 5 is only applicable for the  $\phi = 0.1$  case here, because of the requirement that  $\phi.L > 1$ . The line shows reasonable agreement with the points at high  $A_{part}$ , but is significantly higher at lower values. It is likely that one of the approximations used in the derivation breaks down, particularly as the equations give physically impossible values of  $Q_A > 1$  at the lowest  $A_{part}$  values. The model of equations 6-7 gives an almost linear dependence of  $Q_A$  on  $A_{part}$ . By appropriate choice of the parameter  $k.\lambda^2$ .i.c, this line can be made to agree with the simulation points and the model of equations 1-3 over the low  $A_{part}$  range. However, it would seem that the model of equations 6 and 7 cannot hold throughout

the range of input values studied here. One relevant factor may be that the derivations of both these alternative models seem to assume that the numbers of particles encountered by a light ray can be approximated by the normal distribution. This will only be correct where the mean numbers are large – in many cases low numbers and a Poisson distribution will hold.

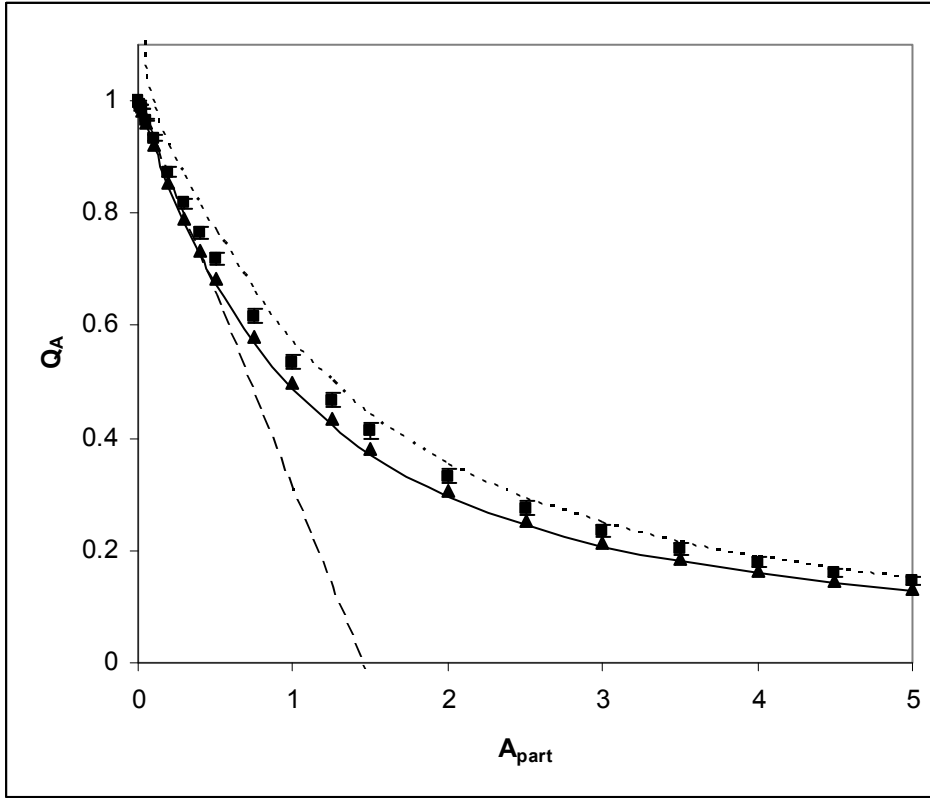


Fig. 2. Predicted QA vales from simulation and literature equations.

Simulations for  $L = 20$ , with  $\phi$  of 0.01 (triangles) and 0.1 (squares). Most error bars are smaller than the size of the points, but they are just visible for the square points at medium  $A_{part}$  values. Lines show results from equations 1-3 (solid); 4 and 5, with  $\phi.L = 2$  and  $N_{ch} = 100$  (dotted); 6 and 7, with  $\phi.L = 0.2$  and  $k.\lambda^2.l.c = 0.25$  (dashed). The latter value was adjusted so that the line agrees with the simulation points and equations 1-3 at the low  $A_{part}$  limit.

No significant effects on the simulation results were found on increasing  $L$ , until  $\phi.L$  values were greater than 2. After that,  $Q_A$  values seemed to become larger for the higher  $A_{part}$  values, although the standard deviations also increased substantially. In this range  $A_{sol}$  and  $A_{sus}$  reached values beyond the normally measurable range. Hence this behaviour has not been investigated further.

Turning to  $Q_{CD}$ , the simulation results indicate that the major influence is again  $A_{part}$ , as shown in Fig 3. Just as with  $Q_A$ , there is a small but significant increase in  $Q_{CD}$  on raising  $\phi$  from 0.01 to 0.1. No significant effect of  $CD_{part}$  on  $Q_{CD}$  was detected anywhere in the region studied. Similarly there was no effect of  $L$  until  $\phi.L$  became greater than 2. At larger values there was an indication of higher  $Q_{CD}$  for larger  $A_{part}$  values, although with the same increased standard deviations and excessive  $A_{sus}$  values as for  $Q_A$ . The literature model of equations 1, 2 and 9 agrees well with the simulation results for  $\phi = 0.01$ , indicating again that it holds for the low  $\phi$  limit. The model of equations 6, 7 and 10 can be adjusted to fit in the initial region of more or less linear decline in  $Q_{CD}$ , but cannot describe the curvature at higher  $A_{part}$  values.

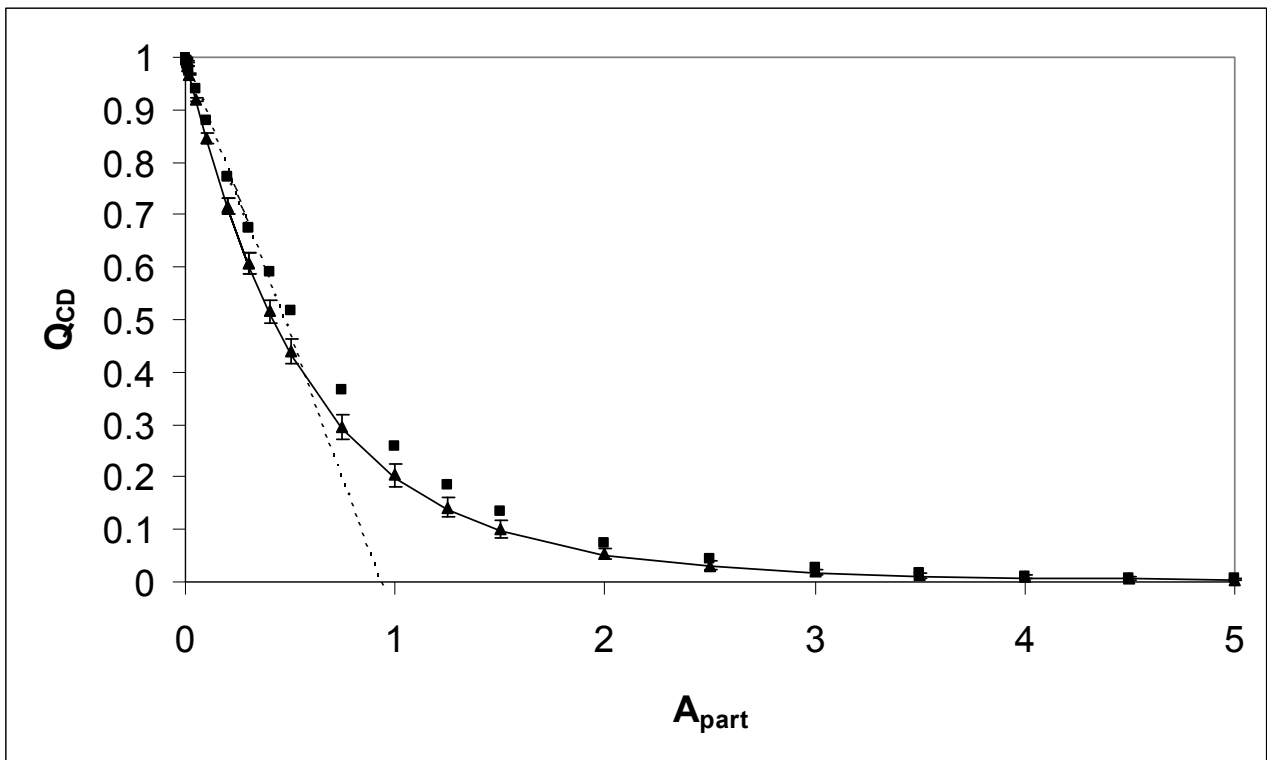


Fig. 3. Predicted  $Q_{CD}$  values from simulation and literature equations.

Simulations for  $L = 2$ , with  $\phi$  of 0.01 (triangles) and 0.1 (squares).  $CD_{part}$  values were 0.0001 for  $A_{part}$  up to 0.3, and 0.02 for  $A_{part}$  of 0.2 and above (the two common points overlap). Error bars are visible for the triangle points at medium  $A_{part}$  values, but otherwise are smaller than the symbols. Lines show results from equations 1, 2 and 9 (solid); 6, 7 and 10, with  $\phi.L = 0.2$  and  $k.\lambda^2.l.c = 0.3$  (dotted). The latter value was adjusted so that the line agrees with the simulation points at the low  $A_{part}$  limit.



In our previous treatment of CD measurements on suspensions of immobilised enzyme particles [11], we used a semi-empirical model based on the assumption that  $Q_{CD}$  was linearly related to the measured absorbance of the suspension. (In this paper we defined the “flattening coefficient” in the same way as Wallace and Mao [5], that is equal to  $(1-Q_{CD})$  as used in the current paper and much of the rest of the literature.) Fig. 4 shows that this approximation is quite good for a range of input values, with  $Q_{CD}$  falling linearly from 1 for  $A_{sus} = 0$ . The slope of the line (the adjustable parameter in our previous treatment) is strongly dependent on the values of  $\phi$  and  $L$ . There may be some deviation from linearity as  $Q_{CD}$  approaches zero, which also corresponds to a predicted maximum possible value of  $A_{sus}$  (because absorption flattening prevents this value being exceeded).

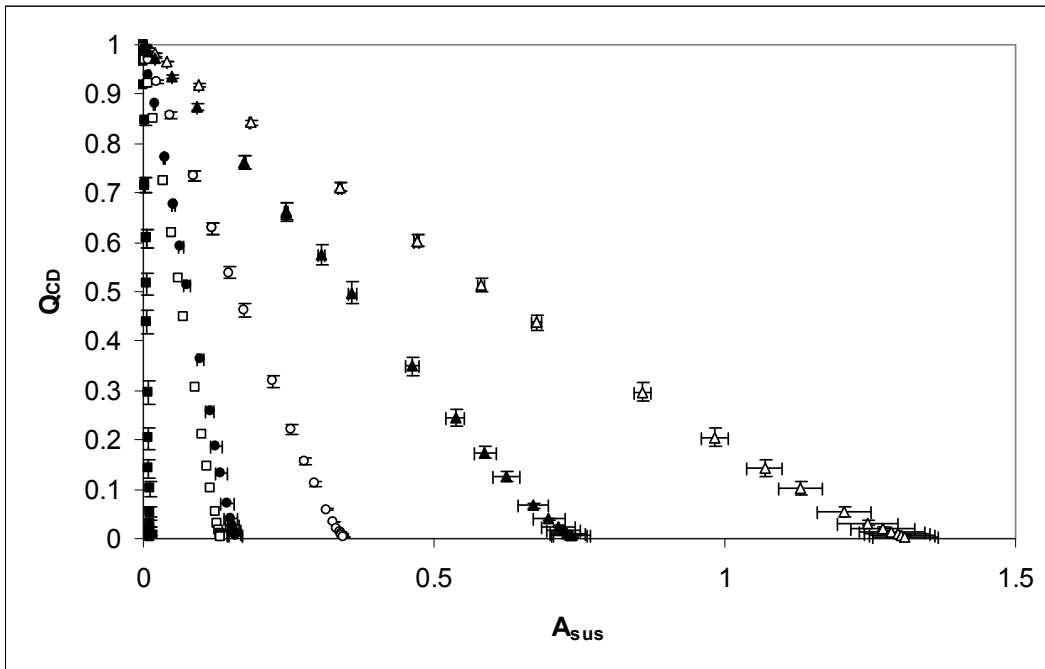


Fig. 4. Relationship between  $Q_{CD}$  and  $A_{sus}$  from simulations.

Points are for the series of  $A_{part}$  values up to 5, and the corresponding  $CD_{part}$  values, as for Fig. 3. The series are for:  $\phi = 0.01$ ,  $L = 2$  (filled squares);  $\phi = 0.01$ ,  $L = 20$  (open squares);  $\phi = 0.1$ ,  $L = 2$  (filled circles);  $\phi = 0.05$ ,  $L = 10$  (open circles);  $\phi = 0.1$ ,  $L = 10$  (filled triangles);  $\phi = 0.01$ ,  $L = 200$  (open triangles). Both x and y error bars are shown, where larger than the size of the points.

To demonstrate the relative ease of relaxing assumptions when using the simulation approach, a particle size range was considered. Instead of all particles being identical in size, they were

given diameters with deviations about the mean, taken randomly from a normal distribution with an appropriate variance. Table 1 compares the  $Q_A$  and  $Q_{CD}$  values found for uniform particle sizes and for a standard deviation of 20% of the mean. As can be seen both  $Q_A$  and  $Q_{CD}$  are significantly smaller when the particles are not equal in size.

Table 1. Effect of particle size distribution on  $Q_A$  and  $Q_{CD}$ .

$\phi$	L	$Q_A$		$Q_{CD}$	
		Monodisperse	Size range	Monodisperse	Size range
0.01	2	$0.499 \pm 0.013$	$0.458 \pm 0.010$	$0.213 \pm 0.014$	$0.174 \pm 0.010$
0.01	200	$0.494 \pm 0.008$	$0.471 \pm 0.009$	$0.200 \pm 0.009$	$0.186 \pm 0.007$
0.1	2	$0.549 \pm 0.003$	$0.501 \pm 0.004$	$0.253 \pm 0.004$	$0.207 \pm 0.004$

Values of  $Q_A$  and  $Q_{CD}$  for  $A_{part} = 1$ , for case with either: a) all particles of identical size, or b) with diameters having a normal distribution with the same mean and a standard deviation of 20% of the mean. Results are shown as mean  $\pm$  standard deviation from 5 replicate runs. All simulations were performed using 64 X 64 light paths, for greater accuracy. All differences between monodisperse particles and those with a size range are statistically significant at levels ranging from 1.2% down to  $10^{-6}\%$ .

The relationship between  $Q_{CD}$  and  $A_{sus}$  suggests an approach to use the simulation to handle experimental data. It will usually be possible to estimate  $\phi$  and L from other measurements on the particle suspension. That should allow construction of a plot of  $Q_{CD}$  vs.  $A_{sus}$  like that of Fig. 4. Then the measured  $A_{sus}$  of the suspension (e.g. obtained from the HT signal on a CD spectropolarimeter) can be used to estimate  $Q_{CD}$  from the plot. Finally this can be used to correct the measured CD signal. In this approach the parameter  $A_{part}$ , as used in the simulation, is effectively determined from the experimentally measured  $A_{sus}$ . Note that it will also be necessary to allow for scattering contributions to measured absorbance, where these are significant, in order to get true  $A_{sus}$  values. Eliminating scattering contributions can be challenging, but there are theoretical and experimental approaches that are useful (e.g. [10]).

To illustrate how the simulation method can be used with experimental data, I have taken a data set from our previously published measurements [11]. The conditions of measurement were used as inputs to a simulation giving the plot of Fig. 5. The HT data from the spectropolarimeter was used to estimate  $A_{\text{sus}}$  values, which were then used to obtain corresponding  $Q_{\text{CD}}$  values, using a smooth interpolation line on Fig. 5. These  $Q_{\text{CD}}$  values are in turn used to correct the CD spectrum, as shown on Fig. 6. The resulting spectrum should be a sounder basis for evaluating the secondary structure in the protein, and other analysis.

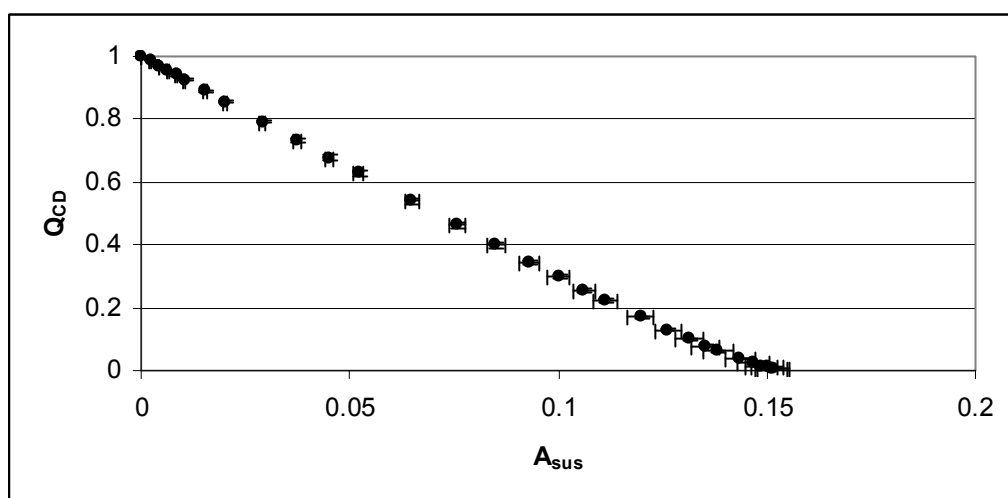


Fig. 5. Relationship between  $Q_{\text{CD}}$  and  $A_{\text{sus}}$  used to correct experimental data.

This plot has been produced by a simulation using input values derived from the conditions of an experimental measurement. A data set from our previously published measurements [11] had been obtained with a pathlength of 0.2 mm, and a silica-subtilisin concentration of 36.7  $\text{mg mL}^{-1}$ . From the particle concentration and an estimate of 0.55 g dry weight per  $\text{cm}^3$  for the porous ( $0.75 \text{ cm}^3 \text{ g}^{-1}$ ) silica particles used,  $\phi$  is calculated as 0.067. From the stated size range of the silica I estimate an L value of 4, and a fractional standard deviation of 0.2 in particle size.

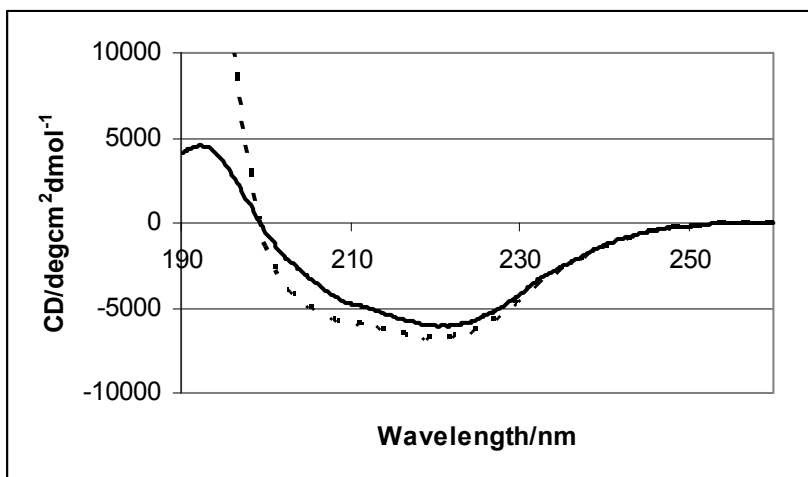


Fig. 6. Correction of circular dichroism spectrum using simulation results.

Measurements were for a suspension of silica-subtilisin in aqueous buffer, and had been converted to the usual CD units using the measured protein concentration in the cell (solid line) [11]. The output for the applied high tension (HT) voltage from the spectropolarimeter was used to estimate the spectrum of  $A_{\text{sus}}$  values for this sample (with some allowance for scattering using the HT data for a suspension of the same silica particles without enzyme immobilised on them). These  $A_{\text{sus}}$  values were then used to obtain corresponding  $Q_{\text{CD}}$  values, using Fig. 5. Finally the table of  $Q_{\text{CD}}$  values was used to produce the corrected CD spectrum (dotted line), calculated as the measured CD divided by  $Q_{\text{CD}}$ . The “corrected” line is not shown at the shortest wavelengths, as here the estimated values of  $Q_{\text{CD}}$  become very small, so that small absolute errors in them will have major effects on the size of the correction, and the results are probably not reliable.

## CONCLUSION

A simulation approach is an effective method to estimate the extent of flattening when making absorption or CD measurements on particle suspensions.

## REFERENCES

- [1] L.N.M. Duysens, The Flattening Of The Absorption Spectrum Of Suspensions, As Compared To That Of Solutions. *Biochimica et Biophysica Acta* 19 (1956) 1-12.

- [2]D.J. Gordon, and G. Holzwarth, Artifacts In The Measured Optical Activity Of Membrane Suspensions. *Archives Of Biochemistry And Biophysics* 143 (1971) 481-488.
- [3]D.W. Urry, Protein Conformation In Biomembranes: Optical Rotation And Absorption Of Membrane Suspensions. *Biochimica et Biophysica Acta* 265 (1972) 115-168.
- [4]P. Latimer, The deconvolution of absorption spectra of green plant materials - improved corrections for the sieve effect. *Photochemistry and Photobiology* 38 (1983) 731-734.
- [5]B.A. Wallace, and D. Mao, Circular-dichroism analyses of membrane-proteins - an examination of differential light-scattering and absorption flattening effects in large membrane-vesicles and membrane sheets. *Analytical Biochemistry* 142 (1984) 317-328.
- [6]C.L. Teeters, J. Eccles, and B.A. Wallace, A Theoretical-Analysis Of The Effects Of Sonication On Differential Absorption Flattening In Suspensions Of Membrane Sheets. *Biophysical Journal* 51 (1987) 527-532.
- [7]B.A. Wallace, and C.L. Teeters, Differential Absorption Flattening Optical Effects Are Significant In The Circular-Dichroism Spectra Of Large Membrane-Fragments. *Biochemistry* 26 (1987) 65-70.
- [8]C. Bustamante, and M.F. Maestre, Statistical effects in the absorption and optical activity of particulate suspensions. *Proc. Natl. Acad. Sci. USA* 85 (1988) 8482-8486.
- [9]P. Wittung, J. Kajanus, M. Kubista, and B.G. Malmstrom, Absorption Flattening In The Optical-Spectra Of Liposome-Entrapped Substances. *FEBS Letters* 352 (1994) 37-40.
- [10]K.R. Naqvi, T.B. Melo, B.B. Raju, T. Javorfi, and G. Garab, Comparison of the absorption spectra of trimers and aggregates of chlorophyll a/b light-harvesting complex LHC II. *Spectrochimica Acta Part a-Molecular and Biomolecular Spectroscopy* 53 (1997) 1925-1936.
- [11]A. Ganesan, N.C. Price, S.M. Kelly, I. Petry, B.D. Moore, and P.J. Halling, Circular dichroism studies of subtilisin Carlsberg immobilised on micron sized silica particles. *Biochimica Et Biophysica Acta-Proteins and Proteomics* 1764 (2006) 1119-1125.

- [12]E. Castiglioni, S. Abbate, G. Longhi, and R. Gangemi, Wavelength shifts in solid-state circular dichroism spectra: A possible explanation. *Chirality* 19 (2007) 491-496.
- [13]E. Castiglioni, S. Abbate, G. Longhi, R. Gangemi, R. Lauceri, and R. Purrello, Absorption flattening as one cause of distortion of circular dichroism spectra of Delta-RuPhen(3).H<sub>2</sub>TPPS complex. *Chirality* 19 (2007) 642-646.
- [14]E. Castiglioni, F. Lebon, G. Longhi, R. Gangemi, and S. Abbate, An operative approach to correct CD spectra distortions due to absorption flattening. *Chirality* 20 (2008) 1047-52.
- [15]S.M. Kelly, T.J. Jess, and N.C. Price, How to study proteins by circular dichroism. *Biochimica et Biophysica Acta* 1751 (2005) 119 - 139.
- [17]B. Sarmiento, D.C. Ferreira, L. Jorgensen, and M. van de Weert, Probing insulin's secondary structure after entrapment into alginate/chitosan nanoparticles. *European Journal of Pharmaceutics and Biopharmaceutics* 65 (2007) 10-17.
- [16]C.S. Braun, G.S. Jas, S. Choosakoonkriang, G.S. Koe, J.G. Smith, and C.R. Middaugh, The structure of DNA within cationic lipid/DNA complexes. *Biophysical Journal* 84 (2003) 1114-1123.
- [18]B. Castillo, V. Bansal, A. Ganesan, P. Halling, F. Secundo, A. Ferrer, K. Griebenow, and G. Barletta, On the activity loss of hydrolases in organic solvents: II. A mechanistic study of subtilisin Carlsberg. *BMC Biotechnology* 6:51 (2006).
- [19]A. Ganesan, A.A. Watkinson, and B.D. Moore, Circular dichroism measurements of the structure and stability of anthrax protective antigen adsorbed onto aluminium adjuvant. *American Association of Pharmaceutical Scientists Journal* 9 (2007) abstract 667. [http://www.aapsj.org/abstracts/NBC\\_2007/NBC07-000667.PDF](http://www.aapsj.org/abstracts/NBC_2007/NBC07-000667.PDF).
- [20]A. Ganesan, A.A. Watkinson, and B.D. Moore, Spectroscopy of insoluble protein aggregates, AAPS - National Biotechnology Conference, abstracts, AAPS, Toronto, Canada, 2008.